Journal of Molecular Catalysis B: Enzymatic 110 (2014) 126–132

Contents lists available at ScienceDirect

Journal of Molecular Catalysis B: Enzymatic

journal homepage: www.elsevier.com/locate/molcatb

Characterization of three novel enzymes with imine reductase activity

M. Gand[a], H. Müller[a], R. Wardenga[b], M. Höhne[a,*]

[a] Institute of Biochemistry, Greifswald University, Felix-Hausdorff-Str. 4, 17487 Greifswald, Germany
[b] Enzymicals AG, Walther-Rathenau-Straße 49a, 17489 Greifswald, Germany

ARTICLE INFO

Article history:
Received 1 July 2014
Received in revised form
23 September 2014
Accepted 28 September 2014
Available online 7 October 2014

Keywords:
Imine reductases
Enzyme catalysis
Chiral secondary amines
Protein function assignment

ABSTRACT

Imine reductases (IRED) are promising catalysts for the synthesis of optically pure secondary cyclic amines. Three novel IREDs from *Paenibacillus elgii* B69, *Streptomyces ipomoeae* 91-03 and *Pseudomonas putida* KT2440 were identified by amino acid or structural similarity search, cloned and recombinantly expressed in *E. coli* and their substrate scope was investigated. Besides the acceptance of cyclic amines, also acyclic amines could be identified as substrates for all IREDs. For the IRED from *P. putida*, a crystal structure (PDB-code 3L6D) is available in the database, but the function of the protein was not investigated so far. This enzyme showed the highest apparent *E*-value of approximately $E_{app} = 52$ for (*R*)-methylpyrrolidine of the IREDs investigated in this study. Thus, an excellent enantiomeric purity of >99% and 97% conversion was reached in a biocatalytic reaction using resting cells after 24 h. Interestingly, a histidine residue could be confirmed as a catalytic residue by mutagenesis, but the residue is placed one turn aside compared to the formally known position of the catalytic Asp187 of *Streptomyces kanamyceticus* IRED.

1. Introduction

A large number of secondary metabolites are composed of chiral secondary amines [1]. Their various physiological activities are explored and utilized by pharmaceutical companies [2]. Hence, many active ingredients of pharmaceuticals represent molecules having one or more stereogenic centres connected to a nitrogen atom. As a consequence, a variety of chemical methods for the enantioselective synthesis of optically pure secondary amines were developed during the last decades, e.g. organocatalytic or metal catalyzed hydrogenation of imines [3,4]. Biocatalysis is more and more accepted as an efficient synthesis strategy for regio- and stereospecific conversions, because it eliminates the use of environmentally toxic heavy metals, enables mild conditions and offers high selectivities [5]. Furthermore, protein engineering allows the fine-tuning of the employed enzymes to broaden their applicability [6]. In contrary to the preparation of primary amines, which can be accessed by various enzymes such as lipases, monoamine oxidases and especially by asymmetric synthesis with transaminases [7–10], for secondary amines there are fewer options: monoamine oxidases allow the deracemization of an amine by oxidizing one enantiomer to the imine, which in turn is reduced non-selectively in situ by chemical means to the amine racemate [11,12]. This leads to the enrichment of the non-reactive enantiomer up to 100%. In a second approach, cyclic *sec*-amines can be obtained in a two-step, one pot reaction if the substrate is carefully chosen: the presence of a halogen, ester or ketone moiety facilitates a spontaneous, intramolecular cyclization via nucleophilic substitution or imine formation [10,13–15]. Dependent on the strategy, a follow-up reductive step is necessary to yield the desired amine. A third option discovered recently are NADPH-dependent imine reductases (IRED) (Fig. 1). So far, only few IREDs were described as recombinant proteins and investigated for the asymmetric synthesis of secondary amines from the corresponding prochiral imines: the (*S*)-selective IRED originating from *Streptomyces* sp. GF3546 (SIR-Sgf3546) [16] and *Streptomyces aurantiacus* (SIR-Sau) [17], and the (*R*)-selective enzymes obtained from *Streptomyces* sp. GF3587 (RIR-Sgf3587) [18] and *Streptomyces kanamyceticus* (RIR-Ska). Crystal structures were solved for SIR-Sgf3546, SIR-Sau, and RIR-Ska [17,19]. During the revision of this manuscript, three additional enzymes were characterized originating from *Streptosporangium roseum* DSM 43021 (RIR-Sro), *Streptomyces turgidiscabies* (RIR-Stu) and *Paenibacillus elgii* B69 (SIR-Pel) [20]. The latter enzyme is one of the proteins that we characterized in detail in this study. Furthermore, the group of Thomas Ward designed artificial metalloenzymes that facilitate the reduction of imines by transfer hydrogenation [21,22].

* Corresponding author. Tel.: +49 3834 86 22832; fax: +49 3834 86 794367.
E-mail addresses: rainer.wardenga@enzymicals.com (R. Wardenga), Matthias.Hoehne@uni-greifswald.de (M. Höhne).

http://dx.doi.org/10.1016/j.molcatb.2014.09.017
1381-1177/

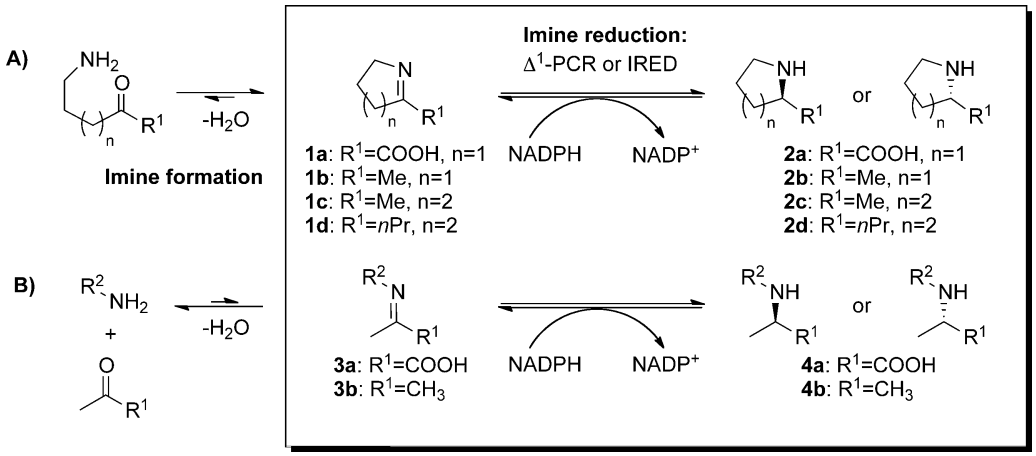

Fig. 1. Enzymatic imine reduction. Δ^1-Pyrrolin-carboxylate reductase (Δ^1-PCR) catalyzes the reduction of cyclic imines (reaction A) or acyclic imines (reaction B), R^1=COOH, n = 1–2. Isolated imine reductases (IRED) reduce the analogous cyclic substrates where R^1 is an alkyl substituent, e.g. a methyl group, and n = 1–3. The question, whether IREDs also act on acyclic substrates (reaction B) is addressed in this study. As the equilibrium favors the hydrolysis of acyclic imines in water (compared to the fairly stable cyclic imines), oxidative deamination of acyclic secondary amines is chosen in initial screening reactions (reverse reaction).

The main challenges for applying IREDs in biocatalysis are (i) only few enzymes are available, (ii) they display a low activity and (iii) some enzymes are reported to show a narrow substrate specificity, especially the (*R*)-selective imine reductase from *Streptomyces* GF3587 (RIR-Sgf3587) [18]. It was suggested earlier that the 'true' natural substrate has not yet been identified [19], or that imine reduction might be a promiscuous activity.

To address the above-mentioned problems, we characterized three proteins similar in sequence or structure to RIR-Ska or SIR-Sgf3546. For their characterization, we screened a broad panel of possible substrates. Besides the substrates of the hydroxyisobutyrate dehydrogenase superfamily (3-hydroxyisobutyrate, 6-phosphogluconate) and cyclic amines, we also examined various alcohols, ketones, aldehydes, amino acids, *prim*- and *sec*-amines.

An additional question is whether IREDs are restricted towards cyclic imine substrates. In principle, imine formation from a ketone and a primary amine of choice would allow the synthesis of acyclic secondary amines. This would be a desirable reaction. During the preparation of this manuscript, Huber et al. published a proof of principle for the reductive amination of three methyl alkyl ketones with methylamine using SIR-Sgf3546 and SIR-Sau: product formation could be detected with conversions ranging from 0.1% to 9%. However, the enzymes showed a very low catalytic turnover of 1.7 molecules/week for the best substrate. Thus, these enzymes are not yet applicable for preparative reactions at larger scale [17]. Another example is described where whole cells were applied to reduce acyclic imines [23], but a huge cell mass (18 g for 0.18 mmol substrate) was needed and the amino acid sequence of the acting catalyst is unknown. In nature, this synthetic strategy is applied for the synthesis of various secondary amines, such as opines. In this case an α-keto acid reacts with an amino acid and the formed imine is reduced stereoselectively to yield an opine [24]. These products usually contain two or more carboxylate functionalities, but these polar groups are often not desired in pharmaceutically active *sec*-amines. Another reaction yielding secondary amino acids is catalyzed by Δ^1-pyrroline-carboxylate-reductase (Δ^1-PCR), which is involved in proline/lysine metabolism: the cyclic substrate Δ^1-pyrroline-carboxylate **1a** is reduced to proline **2a** (Fig. 1A). Interestingly, Δ^1-PCR also reduces acyclic imines like **3a** formed by in situ condensation of α-keto acids like pyruvate with methyl- and ethylamine to the *N*-alkylated α-amino acid **4a** as a side reaction [25] (Fig. 1B). As the model substrate of IREDs, 2-methylpyrroline **1b**, differs from **1a** only by the replacement of the carboxylic acid group by an alkyl substituent, we hypothesized that IREDs could also be active towards the analogous acyclic substrates **3b** and **4b** (Fig. 1B). Therefore, a second aim of this study was to investigate, whether IREDs are able to perform this reaction either as kinetic resolution, or preferentially, in an asymmetric synthesis by generating a stereocenter via reductive amination.

2. Methods and materials

2.1. General

All chemicals were purchased from Fluka (Buchs, Switzerland), Sigma (Steinheim, Germany), Carl-Roth (Karlsruhe, Germany) and Merck (Darmstadt, Germany). The pSGX3 plasmid bearing an insert of a putative reductase with unknown function, (NCBI Gene identification number GI: 283807276, PDB-accession code 3L6D) was kindly provided by the New York Structural Genomics Research Consortium, Department of Biochemistry of Albert Einstein College of Medicine, New York, USA). The genes of the previously described imine reductases SIR-Sgf3546 (GI: 460838082) and RIR-Sgf3587 (GI: 505423772) and two putative reductases identified by BLAST search (GIs: 498183793 and 496688866) were ordered as synthetic genes (GenScript, Piscataway, USA) as subcloned constructs in the pET28b(+) vector, which creates a *N*-terminal His_6-tag for purification purposes. 2-Methylpiperideine was synthesized according to Leipold et al. [26] and for the synthesis of 2-propylpiperideine, the same synthesis procedure was adapted (compare Section 1.1, supplementary information).

2.2. Protein biosynthesis and purification

Kanamycin was used in all cultivations as antibiotic. In a typical procedure, *E. coli* BL21 (DE3) cells transformed with pET28b_IRED were inoculated in LB medium from an overnight culture (1:100, v/v) and were grown at 30 °C until an OD_{600} of 0.2–0.5 was reached. Protein expression was initiated by the addition of IPTG to a final concentration of 0.2 mM. Eight hours after induction, the cells were harvested (4000 g, 4 °C, 10 min) and resuspended in sodium phosphate buffer (50 mM, pH 7.5). The cells were lysed with a French press (Thermo Fisher Scientific, Waltheim, MA, USA) and centrifuged to separate the cell debris from the soluble protein. The His_6-tagged IREDs were purified by metal affinity chromatography using an ÄKTA purifier (GE Healthcare, Chalfont St Giles, UK) with a HisTrap™ FF 5 mL column (GE Healthcare). In a

second step, the IREDs were desalted using Centricon filters (15 mL) with a molecular weight limit of 30 kDa (Merck Millipore, Billerica, MA, USA). The purified enzymes were washed three times with 7.5 mL sodium phosphate buffer (50 mM, pH 7.5) to remove imidazole and NaCl. Finally, the purified proteins were concentrated by reducing the volume to ~2 mL. The purity was evaluated with SDS-PAGE, while the protein content was measured with the Bradford assay [27].

2.3. Determination of enzyme activity

The activities of the purified IREDs were determined from a liquid-phase spectrophotometric assay (Tecan infinite M200 pro, Männedorf, Swiss) monitoring the change of NADPH concentration at 340 nm ($\varepsilon = 6.22\ mM^{-1}\ cm^{-1}$). Reaction mixtures contained buffer (100 mM, sodium phosphate pH 7.5 for the reduction or glycine–NaOH pH 10.5 for the oxidation), 0.2 mM NADPH or 0.2 mM $NADP^+$ for the reduction or oxidation, respectively, in the presence of 5% (v/v) DMSO as cosolvent, and the substrate at the desired concentration. The reaction was started by adding the purified enzyme to the mixture. The reactions were performed at room temperature. One unit is defined as the amount of protein that oxidizes 1 μmol NADPH/min. Controls were done using the same reaction composition but by substitution of enzyme or substrate with buffer. The reported activities are the mean of three purifications (from independent cultivations), each measured in triplicates.

Biotransformations: oxidative deamination of *rac*-*N*-methyl-1-phenylethylamine was performed at 30 °C and 1000 rpm (Eppendorf thermomixer, Hamburg, Germany) in sodium phosphate buffer (100 mM, pH 8) using purified IRED RIR-Sip (4.5 mg/mL). The reaction mixtures typically contained 5 mM substrate, 5% (v/v) DMSO and 5 mM $NADP^+$. 200 μL aliquots were removed in defined time intervals for a period of 24 h. 4-Methylacetophenone was added at 2.5 mM final concentration as internal standard during extraction with two volumes of ethyl acetate followed by drying over anhydrous $MgSO_4$. No derivatization had to be performed. As a negative control, biotransformations were performed in the same way without enzyme. Product analysis (acetophenone, 1-phenylethylamine, *N*-methyl-1-phenylethylamine) was performed by GC–MS analysis with a Shimadzu GC-2010 and GCMS-QP2010 device (Tokyo, Japan), equipped with a HYDRODEX β-TBDAc column (25 m × 0.25 μm, SGE Analytical Science, Milton Keynes, UK). Hydrogen was the carrier gas with a column flow rate of 1.95 mL/min. The analysis was performed with a gradient starting at 65 °C for 40 min and then 1 °C/min to 100 °C followed by 20 °C/min to 180 °C for 5 min. The retention times were as following: 4-methylacetophenone (standard), 75.25 min; acetophenone, 54.5 min; (*S*)-(+)-*N*-methyl-1-phenylethylamine, 32.5 min; (*R*)-(−)-*N*-methyl-1-phenylethylamine 35.5 min, (*R*)-1-phenylethylamine 60.2 min, (*S*)-1-phenylethylamine 56 min.

Whole cell biotransformations were performed at 30 °C and 1000 rpm in sodium phosphate buffer (100 mM, pH 7.0) by using freshly harvested resting cells of *E. coli* BL21 (DE3) expressing an IRED at a final OD_{600nm} of 90. The reaction mixtures contained 2.5 or 5 mM imine and 50 mM of glucose.

Samples were taken after different time points, basified with 20 vol% 10 M NaOH, three times extracted by using 0.5 reaction volumes dichloromethane, containing 2.5 mM 4-methylacetophenone as internal standard, and used directly for GC analysis. Two modified biotransformations were performed as negative controls in the same way as described above using (i) BL21 cells lacking the expression plasmid or (ii) performing the reaction without cells. For calibrating the GC analysis and proof of product stability under reaction conditions, buffered solutions with different concentrations of imines and amines were prepared and measured.

GC–MS analysis was performed by the same equipment mentioned above. Hydrogen was the carrier gas. The injection volumes were 1.5 μL.

Analysis of **1b** and **2b** was performed starting at 60 °C for 15 min followed by an increment of 24 °C/min to 120 °C followed by a 2 min hold. The retention times were assigned using commercial standards: (*S*)-**2b**, 7.5 min; (*R*)-**2b** 9.0 min; **1b**, 16.5 min; 4-methylacetophenone (standard), 16.5 min. The column flow rate was of 1.96 mL/min.

For **1c** and **2c** the following temperature programme was applied: 50 °C for 15 min followed by an increment of 24 °C/min to 120 °C followed by a 2 min hold. The retention times were as following: (*R*)-**2c**, 10.5 min; (*S*)-**2c**, 13.5 min. The later eluting peak was assigned to the (*S*)-enantiomer of **2c** as it is known that SIR-Sgf3546 produces **2c** with (*S*)-selectivity [26]; 2-methylpiperdeine (**1c**), 18 min; 4-methylacetophenone (standard), 20 min. The flow rate was the same as mentioned above.

Analysis of **1d** and **2d** was performed starting with 50 °C for 10 min followed by an increment of 4 °C/min to 110 °C followed by a 10 min hold and a second increment of 24 °C/min to 180 °C followed by a 2 min hold. The retention times were as following: propylpiperdines, 20.9 min and 21.2 min (near baseline separation); 2-propylpiperideine (**1d**), 26 min; 4-methylacetophenone (standard), 31.3 min. The column flow rate was of 1.00 mL/min.

For site-directed mutagenesis a modified QuikChange® PCR protocol was used according to literature [28], and the product transformed in *E. coli* TOP10 cells to repair the nicked ends. Finally the plasmids were isolated and used to transform BL21 (DE3) for protein expression. A list of the primers used in the present study can be found in the supplementary information (Table S1).

3. Results and discussion

3.1. Identification and expression of novel IREDs

Two proteins from *P. elgii* B69 (IRED-Pel) and *S. ipomoeae* 91-03 (IRED-Sip) were identified from a BLAST search. Both proteins were annotated as 6-phosphogluconate dehydrogenases. IRED-Pel showed 65% sequence identity to the known SIR-Sgf3546 [16] while the IRED-Sip has 55% sequence identity towards the RIR-Sgf3587 [18]. The third protein, a putative reductase from *P. putida*, was chosen from a structural alignment of all available structures of the 3-hydroxyisobutyrate dehydrogenase superfamily containing for example the structures of *S. kanamyceticus* (*R*)-selective imine reductase (RIR-Ska) [PDB-code 3ZHB], β-hydroxyl acid dehydrogenase [PDB-code 3CKY], tartronate semialdehyde reductase [PDB-code 1VPD], and 6-phosphogluconate dehydrogenase [PDB-code 4GWP] [29–31]. A remarkable structural difference of RIR-Ska to proteins with other enzyme activities of this superfamily is the dimer formation by reciprocal domain swapping between two subunits [19]. Interestingly, the phenomenon of domain sharing is also observed in the crystal structure of the putative oxidoreductase from *P. putida* (PDB-code 3L6D, compare Fig. S1, supplementary information). This enzyme has not yet been experimentally characterized. It is annotated as 6-phosophogluconate dehydrogenase (Uniprot accession number Q88J51, www.uniprot.org). We have chosen this enzyme for further studies, although the sequence identity to RIR-Ska is low (29%) and instead of the catalytic Asp187 as observed in RIR-Ska, an alanine residue is placed at the structural equivalent position 176 in this oxidoreductase.

The corresponding genes were expressed in *E. coli* and purified by metal affinity chromatography for biochemical characterization and determination of the substrate profile. We found nearly the same amount of protein in the soluble and insoluble fractions (a representative result from a SDS-PAGE and a summary of protein

Table 1
Activity ratio of the used cofactors NADPH/NADH or $NADP^+/NAD^+$. The oxidation was performed with 20 mM (*R*)- or (*S*)-**2b** at pH 10.5 in 100 mM glycine–NaOH buffer. The reduction was done with 20 mM **1b** at pH 7.5 in 100 mM sodium phosphate buffer.

Reaction direction	RIR-Sip	SIR-Pel	RIR-Ppu (3L6D)
Oxidation	6.5	42	7
Reduction	85	4.7	17.5

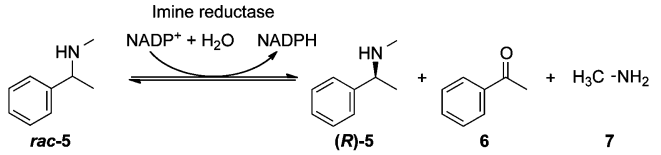

Fig. 2. Intended kinetic resolution of *N*-methyl-1-phenylethylamine catalyzed by IRED.

yields can be found in Fig. S2 and Table S2, supplementary information).

3.2. Optimization of reaction conditions and cofactor preference

In our first attempts, 2-methylpyrroline **1b** and (*R*)- or (*S*)-2-methylpyrrolidine **2b** were used as model substrates in different buffers using both NADPH and NADH as cofactors (or their oxidized forms). We were pleased to detect imine reduction and amine oxidation for all three purified enzymes. The reductase from *S. ipomoeae* and *P. putida* (3L6D) preferred the (*R*)-enantiomer of **2b** in the oxidative reaction and thus are referred to as (*R*)-selective imine reductases (RIR-Sip and RIR-Ppu) throughout this study. The specific oxidation activities towards (*R*)-**2b** were 16 mU/mg and 23 mU/mg under the selected reaction conditions, respectively. The reductase of *P. elgii* preferred (*S*)-**2b** with an activity of 20 mU/mg and is therefore designated as SIR-Pel.

Prior to the screening of a large panel of different substrates, the pH profiles of the enzymes were investigated to elucidate the optimal reaction conditions to guarantee a maximal sensitivity of the assay: for the oxidation reaction, higher pH-values lead to an increased activity. The most suitable buffer for the SIR-Pel, RIR-Sip and RIR-Ppu was sodium phosphate at pH 8, glycine–NaOH at pH 10.5 or pH 10, respectively (pH profiles see Figs. S3–S5, A, supplementary information). On the contrary, the optimal buffer system for the reduction of imines was sodium phosphate at pH 6–7 (see Figs. S3–S5, B, supplementary information). These results are in line with the previously described RIR-Sgf3587 and SIR-Sgf3546 (see Figs. S3 and S4, C and D, supplementary information). All enzymes showed a varying, but significant preference for the phosphorylated cofactors NADP(H) over NAD(H) (Table 1).

3.3. Substrate profiles and enantioselectivities

For the reduction, 2-methylpyrroline, 2-methylpiperideine and 1-methyl-3,4-dihydroisoquinoline were investigated (Table 2). Towards theses substrates, the identified IREDs of this study showed lower activities compared to the already known enzymes and prefer the six-membered ring substrate **1c** over **1b**.

Six secondary cyclic amines were oxidized by the new enzymes. Compared to SIR-Sgf3546 and RIR-Sgf3587, the new IREDs showed similar substrate profiles, but with lower activities towards most substrates (Table 3). To elucidate the possibility of the enzymes to act on acyclic substrates, we investigated acyclic secondary amines rather than imines as substrates in our first screening, because acyclic imines are not stable in water and rapidly hydrolyze into the amine and ketone (Fig. 1). Notably, nine secondary acyclic amines were converted, but to a different extent (Table 3). The enantioselectivity was first analyzed by comparing the oxidative activities towards (*R*)- and (*S*)-**2b**: RIR-Ppu showed the highest apparent *E*-value of approximately $E_{app} = 52$ for the (*R*)-enantiomer, followed by RIR-Sgf3587 with $E_{app} = 19$. The RIR-Sip showed only a 3 fold higher activity towards the (*R*)-enantiomer. The SIR-Sgf3546 and SIR-Pel have nearly the same preference for the (*S*)-enantiomer with an $E_{app} = 6–7$.

To confirm the reactions and enantioselectivities observed in the photometric assays, we performed the asymmetric reduction of three imines using BL21 resting cells having expressed the IREDs (Table 4). In contrast to the oxidation reaction, perfect enantiomeric excesses were obtained for **2b** and **2c** in the reduction with all enzymes. A similar trend (different enantioselectivities in the oxidation and reduction reactions) was observed earlier for SIR-Sgf3546 [26]. As a third substrate, 2-*n*-propylpiperideine **1d** was investigated, yielding the amine **2d**. The obtained enantiomeric excess was low except for the reaction employing SIR-Pel, where an excellent enantioselectivity, but a very low conversion was detected.

A cyclic secondary amino acid, 2-piperidinecarboxylic acid, could be identified as a substrate for four IREDs with 1–15% activity compared to **2c**. RIR-Ppu is the only enzyme which converts the amino acids L-proline and L-glutamic acid with 32% and 8% activity relative to (*R*)-**2b**. This indicates that the active sites can also accept charged molecules, but with less efficiency.

Interestingly, our attempts to detect activities for various substrates of the following substance classes failed: amino acids (except of L-proline and L-glutamic acid), amines, substrates of structurally similar enzymes (3-hydroxy-2-methyl-propanoic acid, 6-phosphogluconic acid), dihydrofolic acid, aldehydes, ketones or keto acids.

3.4. Towards the kinetic resolution of *N*-methyl-1-phenylethylamine

The slow, but selective activity towards the (*S*)-enantiomer of *N*-methyl-1-phenylethylamine **5** encouraged us to investigate a kinetic resolution (Fig. 2). In biotransformations with *rac*-**5**, we found that acetophenone **6** was formed as main product of the deamination, as confirmed via GC-MS. 1-Phenylethylamine could

Table 2
Specific activities ($mU\,mg^{-1}$) in the NADPH-dependent reduction catalyzed by five different IREDs.[b] Each compound was used at a concentration of 20 mM.

Substance	RIR- Sgf3587	RIR-Sip	SIR-Sgf354	SIR-Pel	RIR-Ppu
2-methylpyrroline	490 ± 62	27 ± 3.4	50 ± 20	20 ± 3	66 ± 36
2-methylpiperideine	1241 ± 563	254 ± 31	57 ± 7.4	37 ± 0.4	n.m.
1-methyl-3,4-dihydroisoquinoline	43 ± 4	4 ± 1.2	10 ± 7.4	9 ± 0.3	–[a]

n.m., not measured.
[a] Minimal activity detectable.
[b] For the following compounds, activity was not detectable for any of the investigated IREDs: aldehydes and ketones (ethanol, butanal, 2-methylbutanal, 3-methylbutanal, hexanal, heptanal, benzaldehyde, 4-pyridinecarboxaldehyde, α-methyl-benzylacetaldehyde, 4-nitrobenzaldehyde, 4-oxo-butanoic acid, 2-octanone, 1-phenylmethyl-3-pyrrolidinone, 2-pyrrolidinone, 2-oxo-1,1-dimethylethyl-1-piperidinecarboxylic acid ester), keto acids (2-oxo-propanoic acid, 2-oxo-butyrate, 3-methyl-2-oxobutyrate, 2-oxo-hexanoate, 4-methyl-2-oxo-pentanoic acid, 2-oxo-pentanedioic acid, 2-oxo-benzylpropanoic acid), 2-[(5-nitro-2-furanyl)methylene]-hydrazinecarboxamide.

Table 3
Specific activities (mU mg^{-1}) in the NADP$^+$-dependent oxidation catalyzed by five different IREDs.[a] Each compound was used at a concentration of 20 mM.

Substance	RIR-Sgf3587	RIR-Sip	SIR-Sgf3546	SIR-Pel	RIR-Ppu
Cyclic amines and cyclic amino acids					
(*S*)-(+)-2-methylpyrrolidine	16 ± 9	5 ± 0.2	14 ± 0.1	20 ± 3.5	0.45 ± 0.05
(*R*)-(-)-2-methylpyrrolidine	280 ± 70	16 ± 1.2	2.4 ± 1.8	2.9 ± 1.2	23 ± 14
2-phenylpyrrolidine	152 ± 23	85 ± 1.6	15 ± 5.2	10 ± 0.1	1.2 ± 0.2
2-methylpiperidine	651 ± 117	171 ± 13.4	33 ± 0.8	22 ± 2.5	16 ± 0.5
2-ethylpiperidine	1412 ± 234	290 ± 42	16 ± 3.8	7 ± 2	37 ± 4
2-propylpiperidine	224 ± 84	194 ± 13.4	11 ± 1.6	3 ± 0.1	28 ± 1.5
1,2,3,4-tetrahydroisoquinoline	n.d.	1.5 ± 0.6	1.9 ± 0.4	0.9 ± 0.2	n.d.
2-piperidinecarboxylic acid	7.2 ± 0.2	1.4 ± 0.6	5 ± 1.2	0.7 ± 0.2	n.d.
L-Proline	n.d.	n.d.	n.d.	n.d.	7.4 ± 0.6
Acyclic amines and amino acids with alkyl groups					
N-methyl-2-propanamine	20 ± 9.6	15 ± 0.8	7 ± 3.1	1.7 ± 0.6	n.d.
N-methyl-2-butanamine	75 ± 15.1	58 ± 9	9 ± 2	3 ± 0.8	1.7 ± 0.2
N-methyl-2-pentanamine	20 ± 8.2	93 ± 3.6	n.d.	0.2 ± 0.1	n.d.
N-methyl-3-pentanamine	480 ± 140	309 ± 13.9	2 ± 1.8	n.d.	n.d.
Diisopropylamine	n.d.	n.d.	n.d.	n.d.	13.5 ± 2
6-methyl-*N*-(1-methylethyl)-2-heptanamine	n.d.	93 ± 3.4	n.d.	0.6 ± 0.2	27 ± 2
L-Glutamic acid	n.d.	n.d.	n.d.	n.d.	1.9 ± 0.3
Acyclic amines with aryl groups					
(*S*)-(-)-*N*-methyl-1-Phenylethylamine	76 ± 3.8	17 ± 0.1	1 ± 0.3	0.9 ± 0.4	1 ± 0.4
(*R*)-(+)-*N*-methyl-1-Phenylethylamine	0.7 ± 0.1	n.d.	n.d.	n.d.	n.d.
N-methyl-1-phenylpropanamine	7 ± 4.2	17 ± 0.8	8 ± 0.7	0.6 ± 0.1	n.d.

n.d., no activity detectable over background (<0.5 mU).

[a] For the following compounds, activity was not detectable for any of the investigated IREDs: amino acids (Gly, D- and L-Ala, L-Ser, L-Val, D-Pro, rac-Asp, L-Gln), amines (R-NH_2 with R = methyl–heptyl, benzyl, cyclohexyl, *i*-propyl, *sec*-butyl; 1- and 2-phenylethylamine, 3-phenylproylamine, 4-phenylbutylamine, *N*1,*N*1-dimethyl-1,4-benzenediamine, 7-amino-4-methyl-2H-1-benzopyran-2-one, diisopropylamine, pyrrolidine, (*S*)-1-(2-pyrrolidinylmethyl)-pyrrolidine, (*R*)- and (*S*)-3-aminopyrrolidine, (*R*)-and (*S*)-3-aminopiperidine), substrates of structurally similar enzymes (3-hydroxy-2-methyl-propanoic acid, 6-phosphogluconic acid), dihydrofolic acid (5 mM).

not be detected, indicating that the hydride was abstracted from the chiral carbon of (*S*)-**5** rather than from the *N*-methyl group. Around 9 ± 1.1% conversion was reached after 24 h. This leads to a detectable enantiomeric excess of (*R*)-**5** of 10%ee$_S$, which represents the maximum value in case that the enzyme shows a perfect enantioselectivity. In the control reaction the formation of acetophenone was less than 0.01%, and no enantiomeric excess was detectable. After a proof of the conversion of **5** as an acyclic substrate, the reductive aminations of **6** with methylamine **7** and the alternative reaction of formaldehyde with phenylethylamine were

Table 4
Reduction of three imines after 24 h using resting cells having expressed IRED.

Imine	RIR-Sgf3587		SIR-Sgf3546		RIR-Sip		SIR-Pel		RIR-Ppu	
	Conversion	%ee	Conversion	%ee	Conversion	%ee	Conversion	%ee	Conversion	%ee
1b[a]	94 ± 1%	(*R*)-99	79 ± 6%	(*S*)-99	99 ± 0.1%	(*R*)-99	98 ± 0.1%	(*S*)-99	97 ± 0.6%	(*R*)-99
1c[a]	76 ± 3%	(*R*)-99	80 ± 1%	(*S*)-99	57 ± 5%	(*R*)-99	68 ± 12%	(*S*)-99	72 ± 9%	(*R*)-99
1d[b]	94 ± 1%	35[c]	20 ± 3%	37[d]	42 ± 2%	67[c]	8 ± 2%	99[d]	7 ± 1%	69[c]

[a] Substrate concentration: 5 mM.
[b] Substrate concentration: 2.5 mM.
[c, d] The absolute configuration could not be assigned. The enantiomer formed in excess elutes [c]at 20.9 or [d]at 21.2 min during GC analysis.

investigated in sodium phosphate buffer pH 7.5 and glycine–NaOH buffer pH 10.5 using the photometric assay. Unfortunately, no consumption of NADPH could be detected, indicating that these reductive aminations are not possible under these conditions.

3.5. Active site residue of the IRED Ppu

During IRED catalyzed imine reduction a hydride of NADPH is transferred to the carbon atom of the C=N double bond of the substrate. Thereby, a proton has to be delivered to the nitrogen atom. Asp187 located on an α-helix is likely to facilitate this protonation step in RIR-Ska, as shown by crystallographic und mutagenesis studies [19]. Two neighbouring leucines (Leu137 and Leu191) form a hydrophobic sandwich and are hypothesized to increase the pK_a value of Asp187. Therefore, the pH-optimum of RIR-Ska is ≈3 pH units above the pK_a value of Asp in solution. In RIR-Ppu (3L6D), however, an alanine replaces the catalytic aspartate at the corresponding position 176. Interestingly, RIR-Ppu features a histidine 180 four amino acids downstream in the amino acid sequence. Thus, this His180 is positioned one turn away, but its imidazole ring occupies a similar direction like the side chain of Asp187 of RIR-Ska. Therefore, it might take over the function as the proton shuttling residue in this enzyme (maybe via a water molecule). Similar to RIR-Ska, the neighbouring residues create a relatively hydrophobic environment, composed by amino acids Met126, Val128, Ile142, Ala176, Leu179, and Phe184. The next polar amino acid, His251, is located at the entrance to the active site cleft of the protein. In between the distance of 9 Å (Cβ-carbon atoms), two water molecules are modelled in the structure (for a comparison of the active sites, see Fig. S6, supplementary information). Nevertheless, the pH-optimum of this enzyme matches the pKa-value of histidine of 6.0. In order to proof the catalytic function of His180, we introduced a valine at this position. The purified H180V mutant showed a tenfold reduced specific residual activity. This confirms our hypothesis that H180 contributes to catalysis in the active site of 3L6D.

3.6. Discussion and outlook

One disadvantage of the chemical transition metal-catalyzed imine hydrogenation methods is the requirement to react the starting ketone with nitrogen sources that contain activated groups, e.g., *N*-aryl, *N*-acetyl or *N*-phosphinoyl [32]. After the reduction step, these activating groups are still present at the nitrogen atom and usually must be removed as they are not part of the desired target structure of the natural product or drug. As stated in a recent assessment of synthetic strategies for amine synthesis, a reaction step efficient solution is required, but not available at the moment [32]. Hence, the enzymatic enantioselective reduction of imines is a desirable target reaction to prepare chiral secondary amines, and a large toolbox of enzymes acting on different substrates is desired. Consequently, this study aimed to identify novel imine reductases in protein sequence databases, which can be applied for biocatalytic synthesis of secondary amines. Two of the IREDs investigated in this study, RIR-Sip and SIR-Pel, show a high sequence similarity to RIR-Sgf3587 or SIR-Sgf3546, respectively, and their enantiopreference matched that of the respective enzyme used as search query. However, they showed lower activities towards the investigated substrates. A crystal structure containing both $NADP^+$ and an imine substrate is still missing, and because of this lack of high quality structural information the molecular basis of activity and substrate specificity is poorly understood. This limits the success of in silico discovery of IREDs with preferably high activity towards a desired substrate. Besides the already known subfamilies of (*R*)- and (*S*)-selective IREDs [20], RIR-Ppu represents the first characterized enzyme belonging to a third clade of sequences, which might contain additional IREDs useful for biocatalysis (see Fig. S7, supplementary information). Similar to the discovery and characterization of four amine transaminases [33,34], the crystal structure of RIR-Ppu was deposited in the PDB since 2010, but owing to the lack of experimental characterization, its capability of reducing imines was not recognized until now.

The low activity towards most substrates indicates that the real substrates might not have been identified so far. Although we investigated the oxidation of different amino acids, primary amines as well as the reduction of aldehydes, ketones, lactams, α-keto carboxylic acids and 6-phosphogluconate, no activity could be detected for these substrates (Table 3, footnote). Importantly, we could show that IREDs are active on acyclic secondary amines, although the activities and therefore the conversions are low. Nevertheless, the obtained enantiomeric excess in the oxidation reaction of *rac*-**5** indicates that the enzyme selectively converts the (*R*)-enantiomer. This is a step towards the envisioned synthesis of secondary amines starting from a ketone and primary amine of choice. Unfortunately, an asymmetric reductive amination of ketones was not detectable in this study. However, this reaction could be demonstrated with low conversion and different reaction conditions by Huber et al. [17] very recently. This underlines the potential of IREDs for biocatalysis. A successful reductive amination might be realized as the next step by protein engineering: an optimized variant should promote imine formation and subsequent reduction directly in the active site to overcome the unfavourable equilibrium (hydrolysis).

4. Conclusions

We characterized three new IREDs and confirmed our hypothesis that IREDs are not limited to cyclic amines, as conversion of nine acyclic amines could be confirmed. The RIR-Sip converts one of these acyclic substrates with a higher activity compared to the already known cyclic amines. RIR-Ppu is the first representative enzyme of a new subfamily. For this enzyme a crystal structure is available. The structure reveals a different arrangement of active site residues: a histidine contributes to catalysis, rather than the formerly reported aspartic acid or tyrosine residues. This result underlines the potential of in-depth characterization of enzymes

with unknown functions deposited in the PDB: novel biocatalysts can be discovered and biochemical insights into their structure function relationships can be gained.

Acknowledgements

We thank Uwe T. Bornscheuer for his support and constructive discussions. We thank the New York Structural Genomics Research Consortium for providing the expression plasmid of RIR-Ppu.

Rainer Wardenga thanks the European Union (NewProt project, KBBE-2011- 5, grant no. 289350) for financial support.

Appendix A. Supplementary data

Supplementary material related to this article can be found, in the online version, at http://dx.doi.org/10.1016/j.molcatb.2014.09.017.

References

[1] M. Wink, Phytochemistry 64 (2003) 3–19.
[2] B.W. Cue, J. Zhang, Green Chem. Lett. Rev. 2 (2009) 193–211.
[3] S.Y. Hsieh, M. Binanzer, I. Kreituss, J.W. Bode, Chem. Commun. 48 (2012) 8892–8894.
[4] C. Li, J. Xiao, J. Am. Chem. Soc. 130 (2008) 13208–13209.
[5] K. Buchholz, V. Kasche, U.T. Bornscheuer, Biocatalysts and Enzyme Technology, Wiley-VCH, Weinheim, 2005.
[6] U.T. Bornscheuer, G.W. Huisman, R.J. Kazlauskas, S. Lutz, J.C. Moore, K. Robins, Nature 485 (2012) 185–194.
[7] M. Höhne, S. Kühl, R. Karen, U.T. Bornscheuer, ChemBioChem 9 (2008) 363–365.
[8] D. Ghislieri, N.J. Turner, Top. Catal. 57 (2014) 284–300.
[9] W. Kroutil, E.M. Fischereder, C.S. Fuchs, H. Lechner, F.G. Mutti, D. Pressnitz, A. Rajagopalan, J.H. Sattler, R.C. Simon, E. Siirola, Org. Process. Res. Dev. 17 (2013) 751–759.
[10] H. Kohls, F. Steffen-Munsberg, M. Höhne, Curr. Opin. Chem. Biol. 19 (2014) 180–192.
[11] M. Alexeeva, A. Enright, M.J. Dawson, M. Mahmoudian, N.J. Turner, Angew. Chem. Int. Ed. 41 (2002) 3177–3180.
[12] M. Höhne, U.T. Bornscheuer, ChemCatChem 1 (2009) 42–51.
[13] M. Girardin, S.G. Ouellet, D. Gauvreau, J.C. Moore, G. Hughes, P.N. Devine, P.D. O'Shea, L.-C. Campeau, Org. Process. Res. Dev. 17 (2013) 61–68.
[14] C.K. Savile, J.M. Janey, E.C. Mundorff, J.C. Moore, S. Tam, W.R. Jarvis, J.C. Colbeck, A. Krebber, F.J. Fleitz, J. Brands, P.N. Devine, G.W. Huisman, G.J. Hughes, Science 329 (2010) 305–309.
[15] R.C. Simon, F. Zepeck, W. Kroutil, Chem. Eur. J. 19 (2013) 2859–2865.
[16] K. Mitsukura, T. Kuramoto, T. Yoshida, N. Kimoto, H. Yamamoto, T. Nagasawa, Appl. Microbiol. Biotechnol. 97 (2013) 8079–8086.
[17] T. Huber, L. Schneider, A. Präg, S. Gerhardt, O. Einsle, M. Müller, ChemCatChem 6 (2014) 2248–2252.
[18] K. Mitsukura, M. Suzuki, S. Shinoda, T. Kuramoto, T. Yoshida, T. Nagasawa, Biosci. Biotechnol. Biochem. 75 (2011) 1778–1782.
[19] M. Rodríguez-Mata, A. Frank, E. Wells, F. Leipold, N.J. Turner, S. Hart, J.P. Turkenburg, G. Grogan, ChemBioChem 14 (2013) 1372–1379.
[20] P.N. Scheller, S. Fademrecht, S. Hofelzer, J. Pleiss, F. Leipold, N.J. Turner, B.M. Nestl, B. Hauer, ChemBioChem (2014).
[21] M. Genz, V. Köhler, M. Krauss, D. Singer, R. Hoffmann, T.R. Ward, N. Sträter, ChemCatChem 6 (2014) 736–740.
[22] J.M. Zimbron, T. Heinisch, M. Schmid, D. Hamels, E.S. Nogueira, T. Schirmer, T.R. Ward, J. Am. Chem. Soc. 135 (2013) 5384–5388.
[23] T. Vaijayanthi, A. Chadha, Tetrahedron: Asymmetry 19 (2008) 93–96.
[24] S.H. Smits, A. Mueller, L. Schmitt, M.K. Grieshaber, J. Mol. Biol. 381 (2008) 200–211.
[25] H. Muramatsu, H. Mihara, R. Kakutani, M. Yasuda, M. Ueda, T. Kurihara, N. Esaki, J. Biol. Chem. 280 (2005) 5329–5335.
[26] F. Leipold, S. Hussain, D. Ghislieri, N.J. Turner, ChemCatChem 5 (2013) 3505–3508.
[27] M.M. Bradford, Anal. Biochem. 72 (1976) 248–254.
[28] A. Nobili, M.G. Gall, I.V. Pavlidis, M.L. Thompson, M. Schmidt, U.T. Bornscheuer, FEBS J. 280 (2013) 3084–3093.
[29] S. Reitz, A. Alhapel, L.O. Essen, A.J. Pierik, J. Mol. Biol. 382 (2008) 802–811.
[30] J. Osipiuk, M. Zhou, S. Moy, F. Collart, A. Joachimiak, J. Struct. Funct. Genomics 10 (2009) 249–253.
[31] T. Hitosugi, L. Zhou, S. Elf, J. Fan, H.B. Kang, J.H. Seo, C. Shan, Q. Dai, L. Zhang, J. Xie, T.L. Gu, P. Jin, M. Aleckovic, G. LeRoy, Y. Kang, J.A. Sudderth, R.J. DeBerardinis, C.H. Luan, G.Z. Chen, S. Muller, D.M. Shin, T.K. Owonikoko, S. Lonial, M.L. Arellano, H.J. Khoury, F.R. Khuri, B.H. Lee, K. Ye, T.J. Boggon, S. Kang, C. He, J. Chen, Cancer Cell 22 (2012) 585–600.
[32] T.C. Nugent, M. El-Shazly, Adv. Synth. Catal. 352 (2010) 753–819.
[33] F. Steffen-Munsberg, C. Vickers, A. Thontowi, S. Schätzle, T. Meinhardt, M. Svedendahl Humble, H. Land, P. Berglund, U.T. Bornscheuer, M. Höhne, ChemCatChem 5 (2013) 154–157.
[34] F. Steffen-Munsberg, C. Vickers, A. Thontowi, S. Schätzle, T. Tumlirsch, M. Svedendahl Humble, H. Land, P. Berglund, U.T. Bornscheuer, M. Höhne, ChemCatChem 5 (2013) 150–153.